

***In situ* modulation of the human cardiac ryanodine receptor (hRyR2) by FKBP12.6**

Christopher H. GEORGE¹, Rina SORATHIA, Benedicte M. A. BERTRAND and F. Anthony LAI

Department of Cardiology, Wales Heart Research Institute, University of Wales College of Medicine, Heath Park, Cardiff CF14 4XN, U.K.

The ryanodine receptor complex (RyR), a large oligomeric assembly that functions as a Ca²⁺-release channel in the sarcoplasmic reticulum (SR)/endoplasmic reticulum (ER), comprises four RyR subunits and four FK506-binding proteins (FKBP). The precise mode of interaction and modulation of the cardiac RyR (RyR2) channel by FKBP12/FKBP12.6 remains to be fully defined. We have generated a series of Chinese-hamster ovary (CHO) cell lines stably expressing discrete levels of recombinant human RyR2 (hRyR2) (CHO^{hRyR2}). Confocal microscopy of CHO^{hRyR2} cells co-expressing either FKBP12 or FKBP12.6 demonstrated that FKBP12.6 was sequestered from the cytoplasm to ER membranes as the cellular levels of hRyR2 increased. There was negligible hRyR2-induced subcellular redistribution of FKBP12. The magnitude of Ca²⁺ release in CHO^{hRyR2} cells in response to stimulation by 4-chloro-*m*-cresol was in direct proportion to the expression levels of hRyR2. However, in

CHO^{hRyR2} cells co-expressing FKBP12.6, Ca²⁺ release triggered by the addition of 4-chloro-*m*-cresol was markedly decreased. In contrast, co-expression of FKBP12 did not affect agonist-induced Ca²⁺ release in CHO^{hRyR2} cells. Resting cytoplasmic [Ca²⁺] in CHO^{hRyR2} remained unaltered after co-expression of FKBP12 or FKBP12.6, but estimation of the ER Ca²⁺ load status showed that co-expression of FKBP12.6, but not FKBP12, promoted superfilling of the ER Ca²⁺ store which could not be released by RyR2 after agonist activation. The effects of FKBP12.6 on hRyR2-mediated intracellular Ca²⁺ handling could be antagonized using rapamycin (5 µM). These results suggest that FKBP12.6 associates with hRyR2 *in situ* to modulate precisely the functionality of hRyR2 Ca²⁺-release channel.

Key words: channel regulation, FK506-binding protein, intracellular Ca²⁺ homeostasis, ryanodine receptor.

INTRODUCTION

Calcium release from the endoplasmic reticulum (ER)/sarcoplasmic reticulum (SR) mediated by the ryanodine-sensitive calcium-release channel [ryanodine receptor complex (RyR)] is involved in controlling many cellular processes, including muscle contraction, gene regulation, protein synthesis, apoptosis and memory formation [1]. Three widely expressed isoforms (RyR1–3; RyR1, skeletal-muscle RyR; RyR2, cardiac RyR; RyR3, brain RyR) have been cloned and characterized and all exist as large tetrameric assemblies of RyR subunits (~ 560 kDa) with the N-terminal approx. 80% of the molecule orientated in the cytoplasm and the C-terminal approx. 20% forming the membrane-spanning Ca²⁺-conducting pore. RyR channel function is subject to exquisite levels of modulation via diverse mechanisms, including interaction with accessory proteins [2–4], endogenous small molecule effectors [5], intramolecular interactions [6], the specific arrangement of individual RyR units in the ER/SR membrane [7], covalent modification [8,9] and intracellular redox state [10]. Insight into the specific roles of RyR isoforms has been provided by gene ablation studies [11–13], and the embryonic lethality of RyR2^{-/-} mice highlighted the fundamental importance of RyR2 in early mammalian development [13]. More specifically, its critical role in cardiac function was demonstrated by the recent identification of a number of mutations in the human RyR2 (hRyR2) gene that appear to underlie catecholaminergic polymorphic ventricular tachycardia [14,15] and the findings that

the RyR2 gene locus has been linked with right ventricular hypertrophy and pulmonary hypertension [16].

Co-ordinated calcium release events (sparks) arising from RyR2 activity underpins cardiac-muscle contraction, and defective regulation of RyR2 is implicated in heart failure [17,18]. In particular, defective interaction between RyR2 and FKBP12.6 (FK506-binding protein 12.6) appears to be a key factor in the pathogenesis of heart failure [17,19]. Whereas RyR1 function is modulated only by the FKBP12 isoform, experimental techniques including affinity purification [20], protein exchange [21] and site-directed mutational analysis [22] have suggested that FKBP12.6 selectively interacts with and modulates RyR2. However, these *in vitro* studies have not directly addressed the specific functional role for the RyR2:FKBP12.6 interaction. Confocal microscopy of rat ventricular myocytes demonstrated that the duration and amplitude of Ca²⁺ sparks were altered by treatment of cells with rapamycin [23], a reagent that effectively disrupts the FKBP interaction with RyR [24]. However, this study did not address the specificity of interaction of FKBP12 or FKBP12.6 with RyR. Several other studies have raised questions as to the isoform specificity of the FKBP interaction with RyR2. No skeletal-muscle abnormalities were found in mice deficient in FKBP12, which had normal expression of FKBP12.6 [25]. Surprisingly, these FKBP12^{-/-} mice displayed severe dilated cardiomyopathy, and a functional analysis of purified cardiac SR membranes from these animals revealed that the RyR2 channels were destabilized in the absence of FKBP12, although these observations may be

Abbreviations used: CHO, Chinese-hamster ovary; CMC, 4-chloro-*m*-cresol; ER, endoplasmic reticulum; FKBP, FK506-binding protein; fura 2/AM, fura 2 acetoxymethyl ester; hRyR2, human RyR2; IP₃R, inositol 1,4,5-trisphosphate receptor; KRH, Krebs–Ringer–Hepes buffer; ORF, open reading frame; RyR, ryanodine receptor complex; SERCA, SR/ER Ca²⁺-ATPase; SR, sarcoplasmic reticulum; WT, wild-type.

¹ To whom correspondence should be addressed (e-mail GeorgeCH@cardiff.ac.uk).

indicative of abnormal cardiac development [25]. It has also been reported that RyR2 channel function was not altered after FKBP12.6 removal from purified canine cardiac microsomes [26] and that in membranes isolated from several species, RyR2 interacted with both FKBP12 and FKBP12.6 [27]. Intriguingly, a recent study demonstrated that dysregulated Ca²⁺ release in both male and female FKBP12.6-ablated mice was only associated with abnormal phenotype (cardiac hypertrophy) in male animals [28].

Thus owing to the conflicting nature of the published '*in vitro*' data, and the lack of detailed insight as to the functional role of FKBP binding on molecular events underlying RyR2-mediated Ca²⁺ release in a cellular context, we employed a cell-based strategy to (i) achieve the requisite intracellular conditions permitting *bona fide* FKBP:RyR interaction and (ii) determine a specific functional role of FKBP12.6 or FKBP12 interaction with recombinant hRyR2 on Ca²⁺ handling *in situ*, separated from the accepted limitations of *in vitro* methodologies. Chinese-hamster ovary (CHO) cell lines stably expressing discrete levels of hRyR2 (CHO^{hRyR2}) were co-transfected with either FKBP12 or FKBP12.6 to analyse more precisely the FKBP:RyR protein-protein interactions occurring *in situ* and the functional impact of these interactions on intracellular Ca²⁺ handling. Our results suggest that in living cells, FKBP12 does not associate with hRyR2 and has no effect on the Ca²⁺-releasing functionality of the channel. In contrast, however, a functional interaction between hRyR2 and FKBP12.6 was observed that critically modulated the agonist-stimulated Ca²⁺-release capability of hRyR2 and profoundly altered the Ca²⁺-handling capacity of the cells.

EXPERIMENTAL

Construction of cDNA encoding full-length hRyR2

Overlapping cDNA clones comprising the complete coding sequence of the hRyR2 [29] were assembled to create a single cDNA encoding the entire open reading frame (ORF) of hRyR2. The cDNA fragments were manipulated in pBluescript (Stratagene, Cambridge, U.K.) using Epicurian ColiTM XL1-Blue (Stratagene) as hosts. The subcloning strategy is shown in Figure 1. A 17 bp insert identified in HC9 [29] was deleted by PCR before the incorporation of HC9 into HC12. All restriction enzyme boundaries were verified by automated sequencing. The complete cDNA sequence (−121 to −15335 bp) created by the ligation of HC16 and HC12 was transferred into pcDNA3 (Invitrogen, Paisley, U.K.) using *NotI*–*XhoI* restriction sites generating plasmid pcDNA3/hRyR2 encoding the hRyR2 ORF (14904 bp). Plasmid pcDNA3/hRyR2 was propagated using Epicurian ColiTM XL-10Gold (Stratagene) at 30 °C for ≤ 18 h. Large-scale isolation of pcDNA3/hRyR2 was done using the Wizard Purefection system (Promega, Chilworth, Southampton, U.K.) and plasmid DNA was verified by restriction enzyme mapping. pcDNA3/hRyR2 was stored as single-use aliquots at −80 °C.

Cloning of cDNA encoding human FKBP12 and FKBP12.6

cDNAs corresponding to the ORFs of human FKBP12 and FKBP12.6 were amplified from an adult human cardiac cDNA library (Clontech) using *Pfu* polymerase and the following oligonucleotide pairs: hFKBP12F (TAGCCGCCATGGGAGTGCAGGTGGA)/hFKBP12R (AGTACTCGAGGAGGCCATTCTGTCA) and hFKBP12.6F (TAGGATCCGTGGGACCGCTATGGGCGT)/hFKBP12.6R (GATGCTCGAGTTCC-

TTCCTGCCTTCA) (underlining represents restriction sites) and were subcloned into pCR3 (Invitrogen).

Expression of hRyR2, FKBP12 and FKBP12.6 and generation of CHO^{hRyR2} cell lines

CHO cells were propagated in nutrient Ham's F-12 media, supplemented with 10% (v/v) foetal calf serum, penicillin/streptomycin (100 units/ml and 100 µg/ml respectively) and amphotericin B (2.5 µg/ml). Cells at approx. 80–90% confluency were transfected with plasmids encoding hRyR2, FKBP12 or FKBP12.6 using Lipofectamine2000 according to the manufacturer's instructions (Life Technologies, Basel, Switzerland).

To select CHO^{hRyR2} cells, cells (~6 × 10⁶) were seeded into 10 × 75 cm² flasks in media containing G418 sulphate (500 µg/ml) 48 h post-transfection. After generation of individual colonies (2–3 weeks), cells were serially diluted and individual clones (62 in total) were propagated (6–8 weeks) and assayed for expression of hRyR2 recombinant protein by immunoblotting and by functional Ca²⁺ release in response to 10 mM caffeine and 1 mM 4-chloro-*m*-cresol (4-CMC) as described below.

Confocal detection of recombinant hRyR2, FKBP12 and FKBP12.6

Cells expressing hRyR2, FKBP12 or FKBP12.6 on glass coverslips (4 × 10⁵ cells/22 mm²) were washed in PBS (140 mM NaCl/2.7 mM KCl/10 mM Na₂HPO₄/2 mM NaH₂PO₄; pH 7.4), fixed in paraformaldehyde [4% (v/v) in PBS] for 15 min at 23 °C, and after rehydration in PBS (30 min, 23 °C), cells were permeabilized in Triton X-100 [0.1% (v/v) in PBS] for a further 30 min. Non-specific immunoreactivity was blocked using filtered bovine serum [10% (v/v) in PBS] for 1 h. Coverslips were incubated with primary antibody {rabbit anti-RyR2 [pAb129 (epitope: KAALDFSDAREKKKPKKDSSLSAV)], rabbit anti-RyR [pAb2160 (epitope: FFPAGDCFRKQYEDQLGC)], goat anti-FKBP12/FKBP12.6 [pAbN-19 (Santa Cruz Biotechnology)] and rabbit anti-calreticulin antibody [30]} for 45 min (37 °C) or 15 h (4 °C). Coverslips were washed and incubated with fluorescently linked antibodies [RyR2, goat anti-rabbit F_{ab} conjugated to cy-3 (Amersham Pharmacia Biotech); FKBP, donkey anti-goat conjugated to FITC (Sigma)]. Coverslips were thoroughly washed and mounted on slides using Fluorsave (Calbiochem, Nottingham, U.K.). For non-antibody labelling of expressed hRyR2, a fluorescent derivative of ryanodine, BODIPY[®]-FL-X-ryanodine (10 µM; Molecular Probes, Leiden, The Netherlands) was used. Cells were viewed on a Leitz TCS4D confocal microscope (Leica, Milton Keynes, U.K.) and image acquisition (1024 × 1024 pixel resolution) was controlled using Scanware software (Leica).

Immunoblotting analysis of recombinant hRyR2, FKBP12 and FKBP12.6

To negate the reported effects that detergents, high-speed centrifugation and temperature disrupt the interaction between RyR and FKBP [2,31,32], microsomal fractions were prepared from cells using a detergent-free protocol and low-speed centrifugation; all steps were performed at < 4 °C. Cells (~5 × 10⁶) were pelleted and resuspended in 500 µl of hypo-osmotic buffer (20 mM Tris/HCl, 1 mM EDTA, pH 7.4) supplemented with complete protease inhibitor cocktail (Roche, East Sussex, U.K.). Cells were homogenized through a needle (26 G) and were lysed using freeze-thaw-waterbath sonication with the waterbath maintained at < 4 °C. Nuclei were removed by centrifugation (1500 g, 20 min) and the post-nuclear supernatant (containing membrane

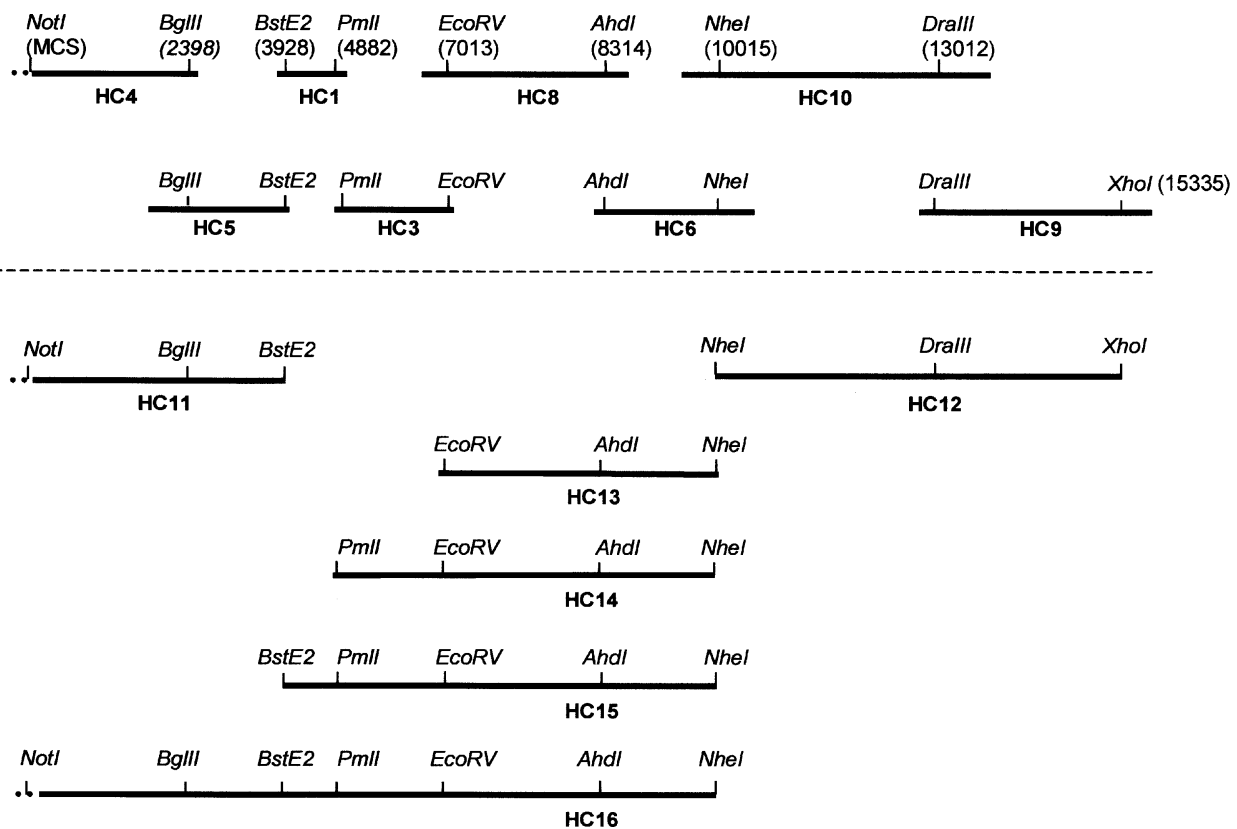


Figure 1 Construction of full-length hRyR2 cDNA

Overlapping cDNA clones (HC1–HC10) encoding the ORF of hRyR2 previously isolated from adult human cardiac cDNA library [29] were sequentially ligated to produce a full-length plasmid. The strategy focussed on extending the N-terminus of hRyR2 (HC11, HC13–HC16), which minimized the number of bacterial propagative stages, involving the more cytotoxic C-terminal approx. 20% of the molecule (HC12). The final ligation of HC16 and HC12 created a single cDNA construct encoding full-length hRyR2 (14904 bp, 4967 amino acids).

and soluble fractions) was concentrated to approx. 50 μ l by vacuum centrifugation (Savant, Farmingdale, NY, U.S.A.). Proteins (100 μ g) were denatured for 30 min at 42 °C in loading buffer [0.1 M Tris/HCl (pH 6.8)/2% (w/v) SDS/2% (w/v) 2-mercaptoethanol/10% (v/v) glycerol/50 μ g/ml Bromophenol Blue], and SDS/PAGE was performed as described previously [29] using 4% (v/v) and 20% (v/v) acrylamide to separate RyR and FKBP samples respectively.

In some experiments, microsomal fractions were obtained from the post-nuclear supernatant (see above) by centrifugation at 20000 *g* for 1 h at 4 °C. Pellets were resuspended in buffer (0.1 M Tris/HCl, pH 7) and in some experiments, rapamycin (5 μ M; 30 min) was added to disrupt FKBP interaction with recombinant hRyR2/endogenous inositol 1,4,5-trisphosphate receptor (IP_3R). After SDS-gel [4% (v/v) acrylamide] electrophoresis, the gel was cut at approximately the 78 kDa marker (Bio-Rad Laboratories) and the upper portion (proteins > 78 kDa) was transferred on to Immobilon-P (PVDF) membrane (Millipore, Watford, Herts., U.K.) as described previously [29]. The lower portion of the gel (< 78 kDa) was transferred on to Immobilon-P membrane for 1 h at 400 mA. Membranes were blocked with 5% (w/v) non-fat dried milk and were incubated with pAb129 (> 78 kDa) and pAbN-19 (< 78 kDa) for 1 h at 23 °C. Membranes were incubated with donkey anti-rabbit (anti-RyR) or rabbit anti-goat (anti-FKBP) antibodies conjugated with horseradish peroxidase, and blots were developed using chemiluminescence (SuperSignal; Pierce, Rockford, IL, U.S.A.).

Densitometric analysis (means \pm S.E.M.) of developed blots was performed using a densitometric scanner (GS-700; Bio-Rad Laboratories) and Quantity One software (Bio-Rad Laboratories).

Fluorimetric analysis of CHO^{hRyR2} cells

Cells were resuspended in Krebs–Ringer–Hepes buffer (KRH + Ca²⁺: 120 mM NaCl/25 mM Hepes/4.8 mM KCl/1.2 mM KH₂PO₄/1.2 mM MgSO₄/5.5 mM glucose/1.3 mM CaCl₂; pH 7.4), containing 4 μ M fura 2 acetoxymethyl ester (fura 2/AM; Molecular Probes) for 45 min at room temperature (23 °C). Immediately before fluorimetric measurements, cells were resuspended (5 \times 10⁵ cells/ml) in prewarmed KRH-Ca²⁺ buffer containing nominal free Ca²⁺ (CaCl₂ replaced with 1 mM EGTA) and transferred to a cuvette continuously stirred at 37 °C (LS-50B; PerkinElmer, Warrington, Cheshire, U.K.). Basal fluorescence levels were measured for 300 s before addition of 4-CMC (1 μ M–10 mM), caffeine (10 mM) or thapsigargin (5 μ M). For procedures in which FKBP:RyR interaction was disrupted, cells were incubated in KRH containing 5 μ M rapamycin (Calbiochem) for 30 min before the start of experiments and for the duration of the experiments. Fluorescence data were converted into [Ca²⁺] as described previously [33].

To estimate intra-ER Ca²⁺ storage capacity, thapsigargin (5 μ M) was added to CHO^{WT} (WT is wild-type) and CHO^{hRyR2} cells maintained in KRH-Ca²⁺ and the total area under the

curve was used to estimate relative ER Ca^{2+} content after the initial thapsigargin-induced efflux of Ca^{2+} . In some experiments, FKBP:RyR interaction was disrupted using rapamycin ($5 \mu\text{M}$) as described above.

Determination of SR/ER Ca^{2+} -ATPase (SERCA) protein levels and ATPase activity in CHO^{hRyR2} cells

Post-nuclear supernatant ($100 \mu\text{g}$) was prepared as described above and immunoblotted for the SERCA using mAb2A7-A1 (Affinity Bioreagents, Golden, CO, U.S.A.). To determine the Ca^{2+} -dependent ATPase activity of SERCA, microsomal fractions were prepared from CHO^{WT} and CHO^{hRyR2} as described previously [34], and the activity of SERCA was determined using the coupled enzyme reaction method of Chu et al. [35]. Briefly, membranes ($50 \mu\text{g}/\text{ml}$) were incubated in reaction buffer (21 mM Mops/ 5 mM sodium azide/ 100 mM KCl/ 3 mM MgCl_2 / 1 mM phosphoenolpyruvate/ 0.2 mM NADH/ 8.4 units pyruvate kinase/ 12 units lactate dehydrogenase/ $50 \mu\text{M}$ CaCl_2) and reactions were started by the addition of ATP (1 mM). The oxidation of NADH was continuously monitored by decreased absorbance at 340 nm (PerkinElmer MBA2000) and was used to calculate Ca^{2+} -dependent ATPase activity as described previously [35].

RESULTS

Plasmid pcDNA3/hRyR2 encoding the full-length hRyR2 ORF of 4967 residues was constructed by sequential ligation of appropriate cDNA fragments (Figure 1), and the contiguous ORF was verified by automated sequencing and restriction enzyme mapping. *Bona fide* plasmid pcDNA3/hRyR2 (20.86 kb) was only consistently propagated using XL-10Gold bacterial strains grown at 30°C for $\leq 18 \text{ h}$. Plasmid pcDNA3/hRyR2 purified from several other commercially available *Escherichia coli* strains (DH5 α , TOP10F' and JM109) gave aberrant restriction digest patterns irrespective of culture temperature (25 – 37°C), duration of culture (15 – 20 h) or culture medium (Luria–Bertani broth, Terrific broth, NZY). Resin-based plasmid DNA purification procedures were associated with significant degradation of the recombinant DNA (results not shown) and thus particle-based purification systems (see the Experimental section) were required for the isolation of intact pcDNA3/hRyR2.

Endogenous RyR isoforms were not detected in CHO^{WT} cells by immunofluorescence analysis using a pan-RyR antibody (pAb-2160; Figure 2A) or a fluorescent derivative of ryanodine, BODIPY[®]-FL-X-ryanodine (Figure 2B). This concurred with previous screening demonstrating a lack of endogenous RyR expression in CHO cells [36]. An antibody raised against the N-terminal 19 residues of FKBP12 which recognizes both FKBP12 and FKBP12.6 showed that CHO^{WT} cells expressed low levels of FKBP12/12.6, which was homogeneously distributed throughout the cytosol, with no evidence of membrane localization (Figure 2C). After transfection of CHO cells with pcDNA3/hRyR2, recombinant hRyR2 was abundantly expressed and was detected using an isoform-specific anti-RyR2 antibody (pAb-129; Figure 2D). The intracellular patterning of hRyR2 displayed a reticular lattice-like distribution that was consistent with ER morphology determined using antibodies raised against calreticulin, an ER-resident protein (Figure 2F). The localization of recombinant hRyR2 protein was also verified using several other antibodies raised against distinct RyR2-specific epitopes (results not shown). Ryanodine binding is critically dependent on the proper folding of RyR and formation of the Ca^{2+} -releasing pore. Importantly, recombinant hRyR2 was detected using BODIPY[®]-FL-X-ryanodine (Figure 2E), indicating correct organization of

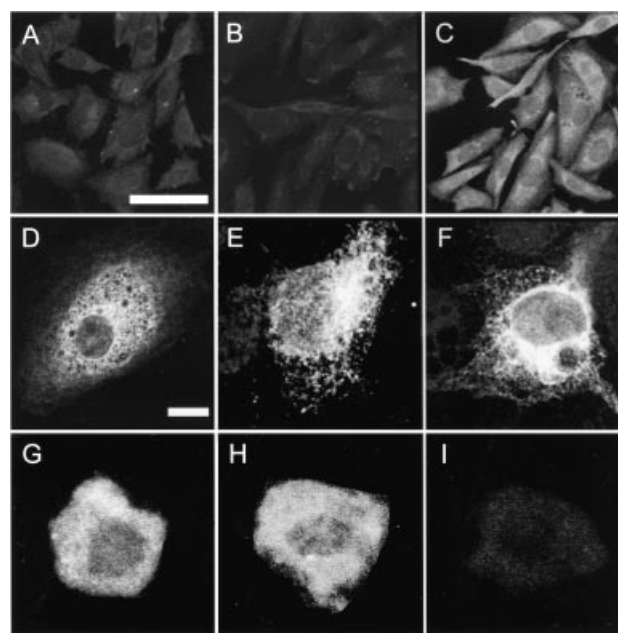


Figure 2 Subcellular localization of recombinant hRyR2, FKBP12 and FKBP12.6 in transfected CHO cells

The endogenous expression status of RyR isoforms in CHO^{WT} cells was determined using a pan-RyR polyclonal antibody (pAb2160) (A) and BODIPY[®]-FL-X-ryanodine (B). The intracellular localization of endogenous FKBP12/FKBP12.6 in CHO^{WT} cells was determined using the FKBP12/12.6-specific antibody pAbN-19 (C). The subcellular localization of recombinant hRyR2 was detected using an RyR2-specific antibody, pAb-129 (D) and also with BODIPY[®]-FL-X-ryanodine (E). Immunostaining of endogenous calreticulin was used to visualize the distribution of the ER network within CHO cells (F). Recombinant human FKBP12 (G) and FKBP12.6 (H) were localized to the cytoplasm. Fluorescent signals due to non-specific binding of fluorescently conjugated antibodies are shown (I). Scale bar represents $50 \mu\text{m}$ (A–C) and $10 \mu\text{m}$ (D–I).

the recombinant protein into intact tetramers. Immunolocalization of recombinant FKBP12 (Figure 2G) or FKBP12.6 (Figure 2H) in CHO cells produced diffuse cytoplasmic localization with no evidence for membrane localization of either FKBP12 or FKBP12.6. Staining of CHO cells transfected with vector alone (pCR3) suggested negligible fluorescent signal attributable to non-specific binding of secondary antibodies (Figure 2I).

In accordance with the immunofluorescence data (Figure 2), immunoblot analysis of CHO^{WT} failed to detect endogenous RyR expression (Figure 3A, lane 4). In contrast, three clonally derived CHO cells stably transfected with hRyR2 (CHO^{#3.2}, CHO^{#3.11} and CHO^{#3.20} and collectively referred to as CHO^{hRyR2}) were found to express discrete levels of hRyR2 protein of the predicted size ($\sim 560 \text{ kDa}$; Figure 3A, lanes 1–3). Relative levels of hRyR2 expression in these transfected cells was determined by densitometry of the approx. 560 kDa band, indicating a normalized rank order of CHO^{#3.2} (1.35) > CHO^{#3.11} (1.2) > CHO^{#3.20} (1). From measurement of relative mobility on immunoblots, the predominant form of FKBP constitutively expressed in both CHO^{WT} and CHO^{hRyR2} was FKBP12, and expression of recombinant hRyR2 did not alter the endogenous levels of FKBP12 in these cells (Figure 3A, lanes 1–4). Consistent with previous reports [25,27], FKBP12.6 was essentially undetectable in post-nuclear fractions CHO^{WT} and CHO^{hRyR2} (Figure 3A, lanes 1–4) and was present only in low abundance in cardiac microsomes (Figure 3A, lane 5). In CHO cells, homeostatic Ca^{2+} signalling events are dependent on

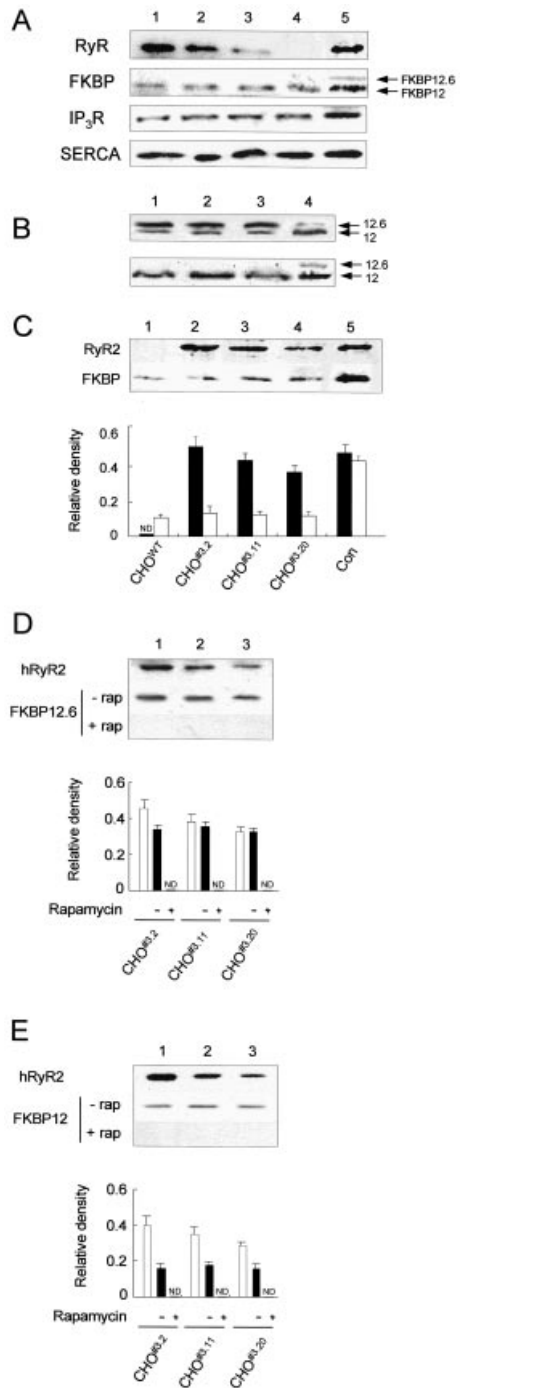


Figure 3 Immunoblot analysis of CHO^{hRyR2} overexpressing FKBP12 and FKBP12.6

(A) Post-nuclear fractions (100 μ g) obtained from CHO^{#3.2}, CHO^{#3.11} and CHO^{#3.20} (lanes 1, 2 and 3 respectively), from CHO^{WT} (lane 4) and from cardiac preparations (RyR, FKBP and SERCA control)/brain preparations (IP₃R control) (lane 5) were immunoblotted for RyR (pAb129), FKBP (N-19), IP₃R (pAb-40) and ER Ca²⁺-ATPase (2A7-A1; Affinity Bioreagents). (B) Immunoblot analysis of post-nuclear supernatants (100 μ g) obtained from CHO^{#3.2}, CHO^{#3.11} and CHO^{#3.20} (lanes 1, 2 and 3 respectively) or cardiac preparations (lane 4) after transfection with recombinant FKBP12.6 (upper panel) or FKBP12 (lower panel). Blots shown are representative of at least three separate experiments. (C) Expression levels of recombinant RyR2 and endogenous FKBP in microsomal fractions (100 μ g) obtained from CHO^{WT} (lane 1), CHO^{#3.2} (lane 2), CHO^{#3.11} (lane 3), CHO^{#3.20} (lane 4) and cardiac microsomes (lane 5). hRyR2 and FKBP were differentially transferred from the same gel [4% (v/v) acrylamide] as described in the Experimental section. (D, E) Immunoblot analysis of microsomal fractions obtained from CHO^{#3.2} (lane 1), CHO^{#3.11} (lane 2) and CHO^{#3.20} (lane 3) transiently co-

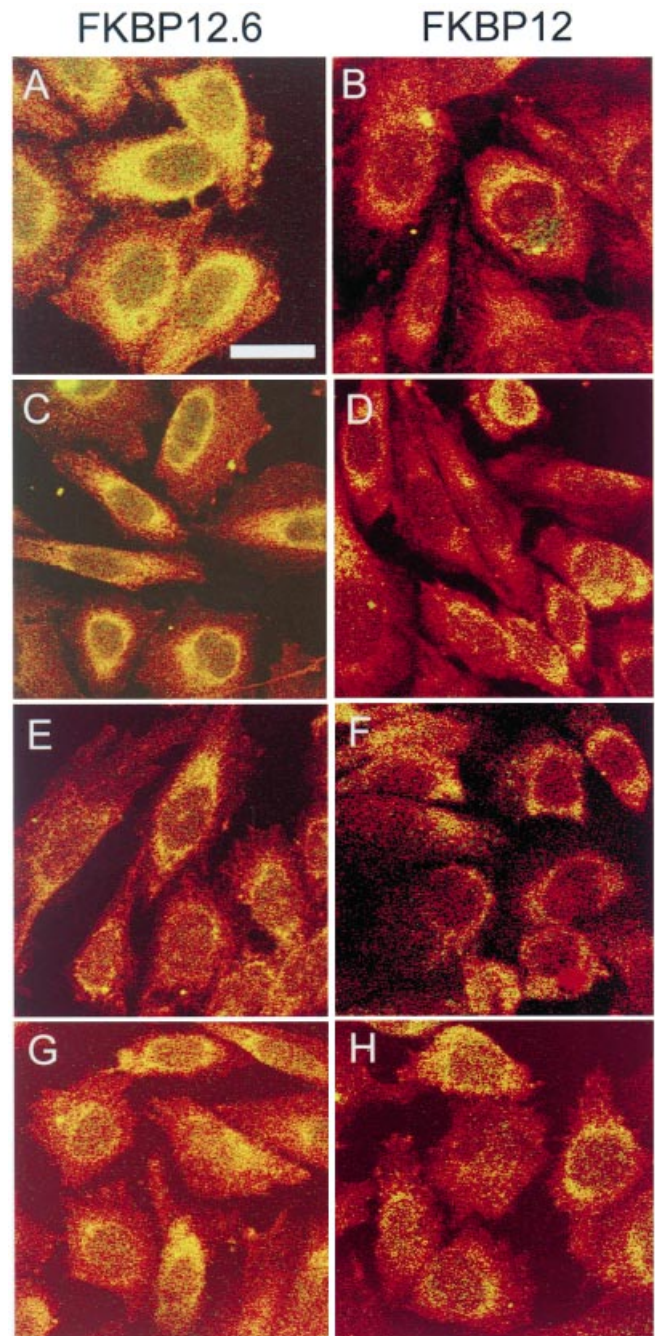


Figure 4 hRyR2 induces a subcellular redistribution of FKBP12.6 but not FKBP12

Confocal laser scanning images of CHO^{hRyR2} depicting intracellular distribution of hRyR2 (red pixels) and FKBP12.6 (green pixels; A, C, E and G) or FKBP12 (green pixels; B, D, F and H) in CHO^{#3.2} (A and B), CHO^{#3.11} (C and D) and CHO^{#3.20} (E and F) cells. Co-incident localization appears yellow. Rapamycin (5 μ M) was added to disrupt RyR:FKBP interaction in CHO^{#3.2} expressing FKBP12.6 (G) or FKBP12 (H). Numerical data relating to this Figure are given in Table 1. Scale bar represents 25 μ m.

expressing FKBP12.6 (D) and FKBP12 (E). Association of FKBP with membranes was determined in the presence (+) or absence (–) of rapamycin (5 μ M). Densitometric analyses of signals (unfilled and filled bars represent hRyR2 and FKBP signals respectively) were performed after the subtraction of background densities surrounding each band and are plotted as mean relative densities \pm S.E.M. ($n = 3$). ND represents immunoblot signals that could not be distinguished from background densities.

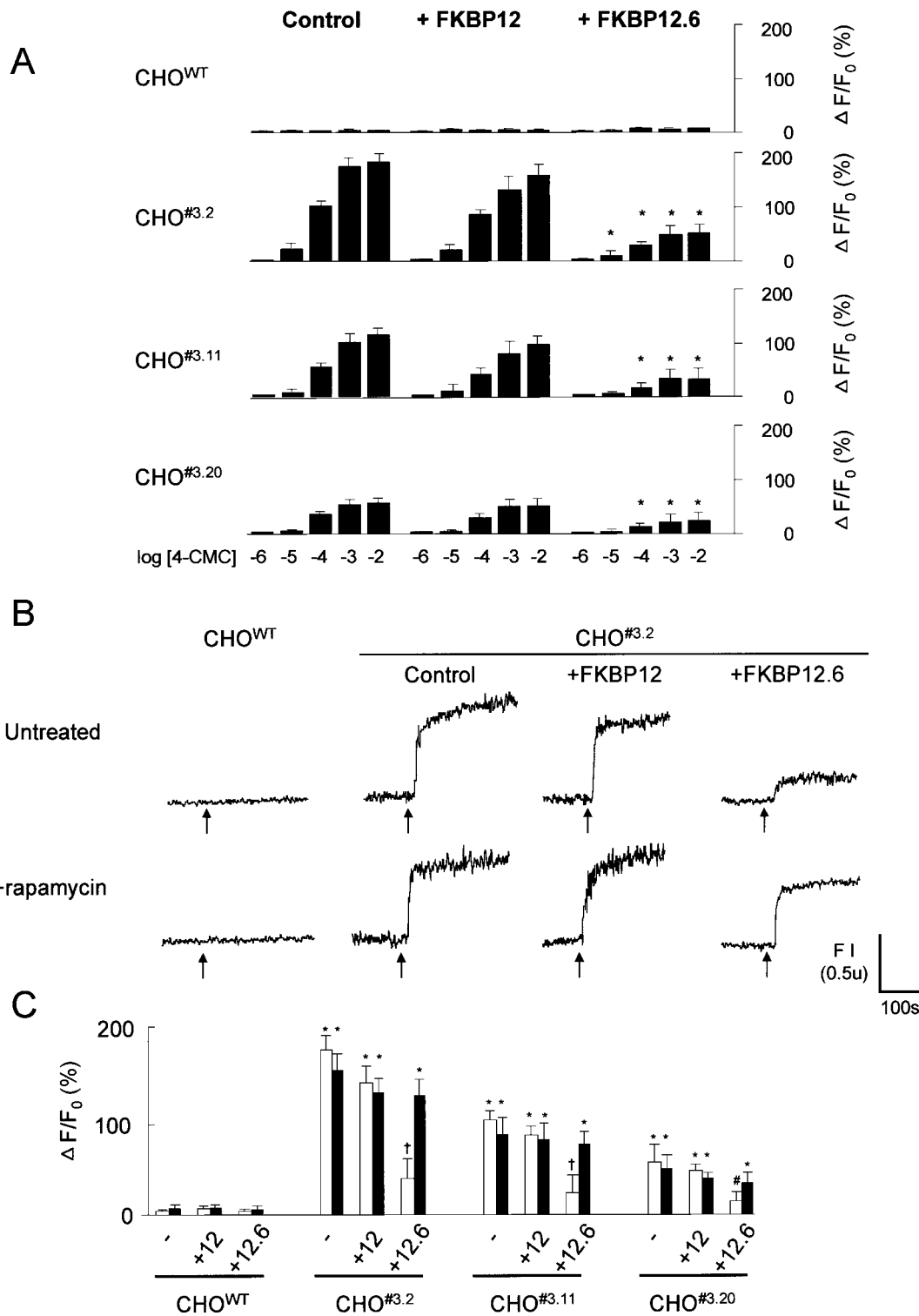


Figure 5 FKBP12.6 inhibits agonist-induced Ca^{2+} release in $\text{CHO}^{\text{hRyR2}}$ cells

(A) RyR-mediated Ca^{2+} release was triggered by addition of 4-CMC ($1 \mu\text{M}$ to 10mM) to CHO^{WT} and $\text{CHO}^{\text{hRyR2}}$ co-expressing FKBP12 or FKBP12.6 and is plotted as the percentage of change in fluorescence after addition of agonist (ΔF) compared with resting measurements (F_0). Data are given as means \pm S.E.M. ($n = 4$). *, $P < 0.005$ when compared with control cells. (B) Ca^{2+} release induced by 4-CMC (1mM) in untreated cells or cells preincubated in rapamycin, as described in the Experimental section. Arrow represents the addition of 4-CMC. The fluorescence intensity FI (ratio 340/380 nm) of the fura 2 signal is shown. (C) 4-CMC-induced Ca^{2+} release in untreated $\text{CHO}^{\text{hRyR2}}$ (—) or co-expressing FKBP12 (+12) or FKBP12.6 (+12.6) isoforms. Untreated cells or those preincubated with rapamycin ($5 \mu\text{M}$) are represented by unfilled and filled bars respectively. Untransfected CHO^{WT} or CHO^{WT} transiently expressing FKBP12 or FKBP12.6 were used as controls. Data are plotted as $\Delta F/F_0$ (%) as given in (A) as means \pm S.E.M. ($n = 6$). *, $P < 0.005$ when compared with control (CHO^{WT}) cells; †, $P < 0.01$ when compared within grouping and with control cells; and #, $P < 0.01$ when compared within grouping.

inositol 1,4,5-trisphosphate-linked mechanisms [37] and in concert with this, IP_3R was readily detected in immunoblots of both CHO^{WT} and CHO^{hRyR2} (using anti- IP_3R antibody pAb-40 [38]). Densitometric analysis of IP_3R immunoblot signals suggested that endogenous expression levels of IP_3R in $CHO^{#3.2}$, $CHO^{#3.11}$ and $CHO^{#3.20}$ (0.81 ± 0.26 , 0.94 ± 0.19 and 1.09 ± 0.2 respectively; lanes 1–3) were similar to that determined in CHO^{WT} (1.00; lane 4) and confirmed that IP_3R expression was independent of hRyR2 expression levels in CHO^{hRyR2} (Figure 3A). Similarly, CHO^{WT} abundantly express the ER Ca^{2+} -ATPase, the levels of which were unaltered after expression of hRyR2 in $CHO^{#3.2}$ (0.91 ± 0.13), $CHO^{#3.11}$ (0.85 ± 0.16) and $CHO^{#3.20}$ (1.13 ± 0.12) when compared with CHO^{WT} (1.00).

Transient transfection of FKBP12.6 and FKBP12 plasmids in CHO^{hRyR2} resulted in a high expression level of recombinant FKBP protein (Figure 3B, upper and lower panels respectively, lanes 1–3). No significant difference was observed between the $CHO^{#3.2}$, $CHO^{#3.11}$ and $CHO^{#3.20}$ cell populations in their relative expression levels of either FKBP12.6 or FKBP12 (Figure 3B). Similarly, the relative levels of recombinant hRyR2 in the various CHO^{hRyR2} cells transiently co-expressing FKBP12.6 or FKBP12 were not altered (results not shown) when compared with the CHO^{hRyR2} cells alone (Figure 3A, top panel). Thus the amount of exogenous FKBP12.6 or FKBP12 present in these cells was not dependent on the level of recombinant hRyR2 expression and vice versa (Figure 3B).

We compared the relative amounts of hRyR2 and FKBP that were associated specifically with membrane fractions (100 μ g) isolated from the CHO^{hRyR2} cells using mild conditions (see the Experimental section) and cardiac muscle. In cardiac microsomes (Figure 3C, lane 5), the RyR2:FKBP ratio was consistently low, due to the relatively high levels of FKBP expression in the heart [21]. In contrast, the RyR2:FKBP ratio in CHO^{hRyR2} cells was high (Figure 3C, lanes 2–4) in simultaneous comparisons performed under identical conditions and was similar to that observed in CHO^{WT} cells (Figure 3C, lane 1). This observation in CHO^{hRyR2} cells suggests that most of the recombinant hRyR2 may not be associated with the FKBP12 [identified as the endogenously expressed FKBP isoform (Figure 3A)] in CHO^{hRyR2} membrane preparations isolated using a protocol that does not disrupt RyR:FKBP interaction [31]. After transfection of the CHO^{hRyR2} cells with FKBP12.6, the hRyR2:FKBP12.6 ratio in microsomal preparations (Figure 3D) approached that seen in cardiac microsomes (Figure 3C, lane 5). The association of FKBP12.6 with hRyR2 containing microsomes was completely abolished after addition of rapamycin (Figure 3D, lower panel), strongly indicative of specific FKBP12.6:RyR2 protein–protein interaction. Figure 3(E) indicates that little recombinant FKBP12 was associated with microsomal membranes isolated from CHO^{hRyR2} cells using mild (detergent-free) conditions when compared with membrane fractions obtained from untransfected (RyR-deficient) CHO^{WT} cells (Figure 3C). It is important to note that these microsomal fractions contain abundant endogenous IP_3R [39] and that protein–protein interaction between FKBP12 and IP_3R is widely reported [40–44]. The interaction between FKBP12 and endogenous microsomal IP_3R was also disrupted by rapamycin (Figure 3E, lower panel). Thus our results suggest that FKBP12 does not interact spatially (Figures 3 and 4) or functionally (Figures 5 and 6) with hRyR2 and, therefore, the presence of FKBP12 in these microsomal fractions is probably due to tight association of recombinant FKBP12 with endogenous IP_3R .

In agreement with the RyR immunoblot data (Figure 3), immunofluorescent detection using pAb129 showed that the rank order of hRyR2 expression in CHO^{hRyR2} cells was

$CHO^{#3.2} > CHO^{#3.11} > CHO^{#3.20}$ (Figure 4, red pixels). The transient expression of FKBP12.6 and FKBP12 observed by immunofluorescence (Figure 4, green pixels) was also consistent with immunoblots (Figure 3) showing comparable expression levels across the CHO^{hRyR2} cell population. Transfection efficiencies of 80–90% were routinely achieved for both FKBP12 and FKBP12.6 and thus nearly all cells simultaneously expressed hRyR2 and FKBP12/FKBP12.6. Comparison of their subcellular distribution revealed a striking difference between FKBP12.6 and FKBP12 in CHO^{hRyR2} . Directly overlaying images that were positively stained for hRyR2 (Figure 4, red pixels) and FKBP12.6 (Figure 4, green pixels) generated images in which co-incident staining appears as yellow pixels (Figure 4). The extent of overlap between hRyR2 and FKBP12.6 increased concomitantly with increasing levels of hRyR2, i.e. increasing co-incident staining of hRyR2 and FKBP12.6 (yellow pixels) followed the pattern of $CHO^{#3.2} > CHO^{#3.11} > CHO^{#3.20}$ (Figures 4A, 4C and Table 1). Since the level of FKBP12.6 and endogenous IP_3R remained unaltered as hRyR2 expression increased (Figures 3B and 3C), the increasing level of co-incident staining as a function of increased hRyR2 expression was interpreted as an indicator of *in situ* association between hRyR2 and FKBP12.6. Rapamycin disrupted the hRyR2:FKBP12.6 interaction (Figure 4G and Table 1). In contrast, analysis of FKBP12 immunofluorescence did not show any correlation with hRyR2 density (Figures 4B, 4D and 4F) and subcellular distribution of FKBP12 remained unaltered after exposure to rapamycin (Figure 4H). Quantitative analysis of pixel overlap with FKBP12 (Table 1) showed the co-incident staining level, ranging from 30 to 32%, was independent of increasing hRyR2 levels, with only a small proportion of this being rapamycin-sensitive (Figure 4 and Table 1). However, FKBP12.6 co-incident staining ranged from 69 to 52%, in concert with relative hRyR2 levels, and up to half of this signal was displaced by rapamycin (Table 1). A persistent basal level of overlapping pixels (20–25%) could not be diminished by increased dose or time of exposure to rapamycin (Figure 4, Table 1) and therefore represented the limiting resolution of our system. Only overlapping pixel values of > 25% were considered to be a reliable indicator of *bona fide* protein–protein association. These results therefore provide *in situ* evidence that hRyR2 expression in CHO cells can cause significant translocation of FKBP12.6, but not FKBP12, from the cytoplasm to the ER.

Fluorimetric Ca^{2+} release assays were performed to assess whether *in situ* association of hRyR2 and FKBP isoforms corresponded to altered agonist-induced intracellular Ca^{2+} -

Table 1 hRyR2 induces a subcellular redistribution of FKBP12.6 but not FKBP12, which is rapamycin-sensitive

Co-incident localization of hRyR2 and FKBP12 or FKBP12.6 in CHO^{hRyR2} is expressed as a percentage of the total intracellular hRyR2 signal (red pixels, Figure 4) and FKBP12 or FKBP12.6 signal (green pixels, Figure 4) that can be directly overlaid (yellow). Values are obtained from image analysis of at least nine images and are given as means \pm S.E.M.

FKBP isoform	Rapamycin	Cell line		
		$CHO^{#3.2}$	$CHO^{#3.11}$	$CHO^{#3.20}$
12.6	–	$69.3 \pm 3.8^*$	$60.6 \pm 4.2^*$	$52.3 \pm 2.7^*$
	+	35.2 ± 5.1	32.1 ± 4.8	34.6 ± 4.3
12	–	32.4 ± 4.2	31.7 ± 3.4	30.3 ± 3.9
	+	25.1 ± 4.1	25.4 ± 4.3	23.6 ± 3.9

* $P < 0.01$.

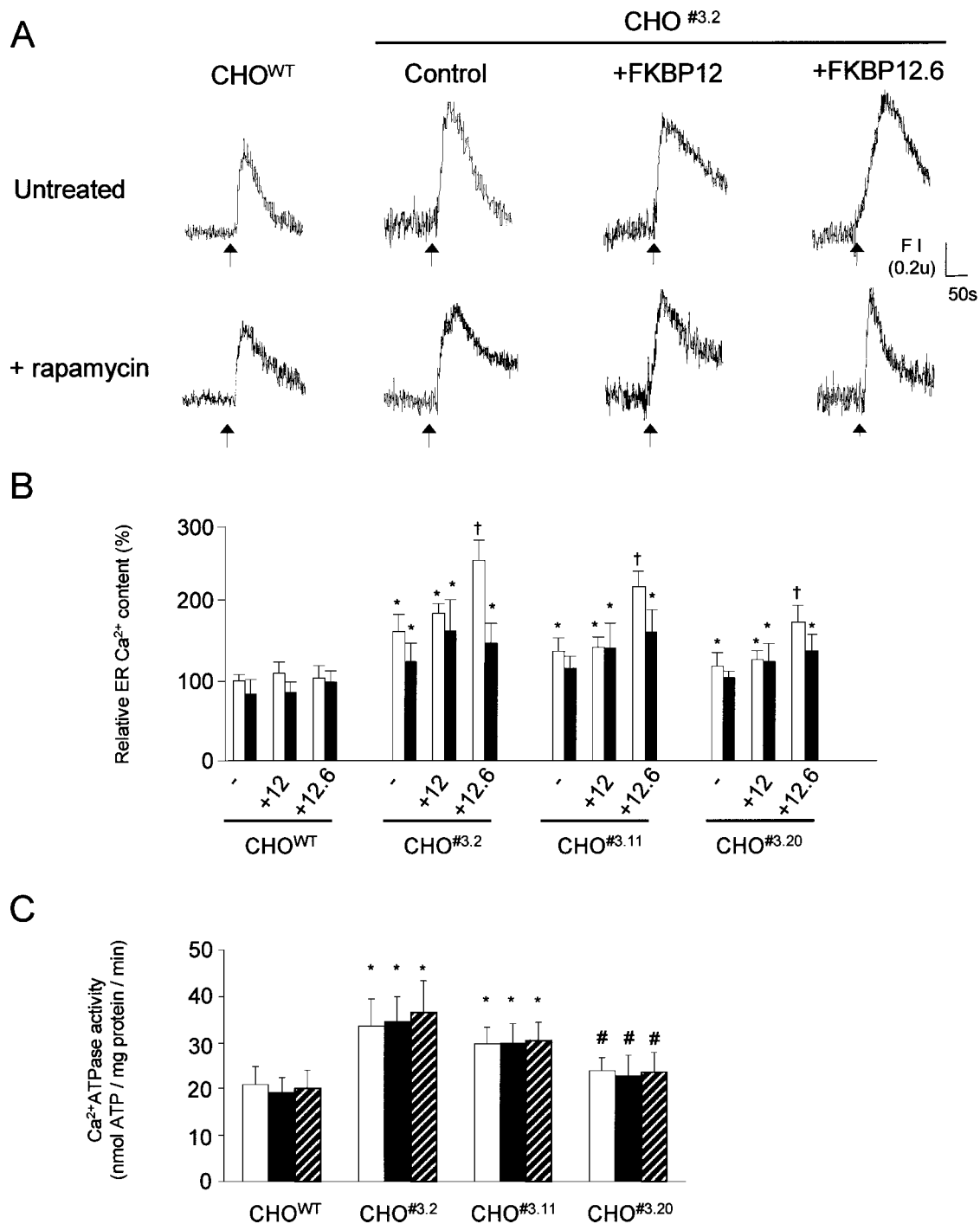


Figure 6 Co-expression of FKBP12.6 potentiates the increased ER Ca²⁺ content in CHO^{hRyR2}

(A) Estimation of relative ER Ca²⁺ content in CHO^{hRyR2} alone or in combination with FKBP12 or FKBP12.6 and the effect of rapamycin treatment on ER Ca²⁺ capacity. Arrow indicates addition of thapsigargin (5 μ M). FI of the fura 2 signal (ratio 340/380 nm) is shown. (B) Estimation of relative ER Ca²⁺ content in CHO^{hRyR2} alone (—) or co-expressing FKBP12 (+12) or FKBP12.6 (+12.6). Filled and unfilled bars represent untreated cells or those preincubated with rapamycin (5 μ M) respectively. Untransfected CHO^{WT} or those transiently transfected with FKBP12 or FKBP12.6 were used as controls. Data are plotted as initial Ca²⁺ released in response to thapsigargin in CHO^{hRyR2} cells normalized to measurements taken in CHO^{WT} cells (100%) and are given as means \pm S.E.M. ($n = 4$). *, $P < 0.01$ when compared with CHO^{WT} cells; †, $P < 0.01$ when compared within grouping and with CHO^{WT} cells. (C) The Ca²⁺-ATPase activity of endogenously expressed SERCA in CHO^{WT} and CHO^{hRyR2} (unfilled bars) and in cells co-expressing FKBP12 (filled bars) or FKBP12.6 (hatched bars) was determined as described in the Experimental section. Data are plotted as means \pm S.E.M. ($n = 4$). *, $P < 0.005$; #, $P < 0.01$ when compared with CHO^{WT}.

release characteristics (Figure 5). Resting [Ca²⁺]_c was similar in CHO^{WT}, CHO^{#3.2}, CHO^{#3.11} and CHO^{#3.20} (88 ± 11 , 108 ± 15 , 103 ± 11 and 94 ± 12 nM respectively; $n = 9$), suggesting that

expression of hRyR2 did not condition the cells to elevated resting [Ca²⁺]_c. RyR-mediated release of Ca²⁺ from the ER was triggered by the addition of 1 μ M–10 mM 4-CMC, a highly selec-

tive and potent agonist of RyR function [45]. CHO^{WT} did not possess a 4-CMC-mobilizable Ca²⁺ store, in agreement with our findings that CHO^{WT} cells do not express RyR (Figures 2 and 3). The addition of 4-CMC to CHO^{hRyR2} produced, in contrast, a rapid, large and sustained Ca²⁺ release consistent with the expression of exogenous hRyR2 (Figures 5A and 5B). The sustained elevation of [Ca²⁺]_c observed after 4-CMC addition to CHO^{hRyR2} (Figure 5B) is a characteristic of 4-CMC-induced RyR Ca²⁺ release [46,47]. The magnitude of 4-CMC-induced Ca²⁺ release in CHO^{hRyR2} was proportional to the expression levels of hRyR2 (Figures 3 and 4). Maximal RyR-mediated Ca²⁺ mobilization was triggered by the addition of ≥ 1 mM 4-CMC to CHO^{hRyR2} (Figure 5A), and 1 mM CMC was used to stimulate hRyR2 Ca²⁺ release in subsequent experiments. Our results also indicate that differences in Ca²⁺ homeostasis observed among CHO^{#3.2}, CHO^{#3.11} and CHO^{#3.20} cell lines occurs directly as a consequence of differential expression of hRyR2 and not as a consequence of receptor reserve. The lack of effect of 4-CMC in CHO^{WT} cells persisted after expression of FKBP12 or FKBP12.6 (Figure 5A). Co-expression of FKBP12 in CHO^{hRyR2} did not alter the dose–response relationship of 4-CMC activation of hRyR2, and FKBP12 had negligible effect on the magnitude of 4-CMC-induced Ca²⁺ release via hRyR2 (Figures 5A and 5C). However, after co-expression of FKBP12.6 in CHO^{hRyR2}, there was a dramatic decrease in the amount of Ca²⁺ that could be mobilized via hRyR2 in response to 4-CMC. For example, in CHO^{#3.2} co-expressing FKBP12.6, 4-CMC-triggered maximal [Ca²⁺]_c was 254 ± 41 nM, compared with 720 ± 47 nM in untransfected CHO^{#3.2} (Figure 5C). It should be noted that despite significantly decreasing hRyR2 Ca²⁺ release in response to 4-CMC, co-expression of FKBP12.6 in CHO^{hRyR2} cells did not alter the dose–response profile of 4-CMC activation (Figure 5A). Rapamycin did not alter resting [Ca²⁺]_c in CHO^{WT} (94 ± 12 nM) or CHO^{#3.2} (110 ± 16 nM), CHO^{#3.11} (104 ± 11 nM) or CHO^{#3.20} (96 ± 9 nM) (*n* = 9) when compared with untreated controls (see above). However, the marked reduction of Ca²⁺ release in hRyR2:FKBP12.6-expressing cells was almost completely reversed when the cells were preincubated with rapamycin (Figures 5B and 5C). Addition of rapamycin to CHO^{hRyR2} cells co-expressing FKBP12 had little effect on 4-CMC-induced Ca²⁺ release (Figures 5B and 5C), strengthening our hypothesis that FKBP12 does not modulate hRyR2 Ca²⁺ release by specific protein–protein interaction. Thus it appeared that FKBP12.6, and not FKBP12, specifically modulated hRyR2 Ca²⁺ release via a rapamycin-sensitive interaction, but the mechanism of FKBP12.6 action on agonist-stimulated hRyR2 was unlikely to be due to FKBP12.6 altering the potency of 4-CMC activation of hRyR2. These results demonstrate a rapamycin-sensitive functional specificity of hRyR2 for the FKBP12.6 isoform in the regulation of Ca²⁺ store release, which may explain the molecular events underlying the phenotypic alterations in FKBP12.6^{-/-} animals [28].

It was important to demonstrate clearly that the FKBP12.6-mediated inhibition of hRyR2 Ca²⁺ release *in situ* (Figure 5) was indeed due to *bona fide* hRyR2:FKBP12.6 protein–protein interaction and did not simply reflect an RyR-independent effect of FKBP12.6 on ER Ca²⁺ status. The ER Ca²⁺ content in CHO^{hRyR2} cells or in those expressing FKBP12.6 or FKBP12, was estimated using thapsigargin, a reagent that can deplete ER Ca²⁺ pools. Interestingly, there was a marked increase in the Ca²⁺ content of the ER in all CHO^{hRyR2} when compared with CHO^{WT} (Figure 6, unfilled bars) and this increase in ER Ca²⁺ load was proportional to the amount of hRyR2 expressed, i.e. Ca²⁺ load CHO^{#3.2} (164 ± 26%) > CHO^{#3.11} (139 ± 21%) > CHO^{#3.20} (118 ± 17%), relative to CHO^{WT} (100%). ER Ca²⁺ load in

CHO^{hRyR2} (Figure 6B, unfilled bars) was markedly augmented by only small increases in RyR2 expression levels (Figure 3A). Co-expression of FKBP12 had negligible effect on the ER Ca²⁺ store in CHO^{hRyR2} cells, but importantly, the ER Ca²⁺ content was greatly augmented upon co-expression of FKBP12.6 (Figures 6A and 6B). This surprising result indicated that the inhibitory interaction of FKBP12.6 with hRyR2 (i.e. decreased hRyR2-mediated Ca²⁺ release in response to 4-CMC) was definitely not underpinned by a general reduction in ER Ca²⁺ load but was in fact associated with a markedly increased ER Ca²⁺ capacity. Thus despite the superloading of ER Ca²⁺ after expression of FKBP12.6 in CHO^{hRyR2} cells, this store could not be released by hRyR2 in response to agonist. As described above, basal [Ca²⁺]_c was not significantly different in CHO^{hRyR2} cells when compared with CHO^{WT}, suggesting that increased ER Ca²⁺ storage capacity as a consequence of hRyR2 overexpression does not condition the cell to increased cytoplasmic [Ca²⁺]_c.

After incubation of CHO^{WT}, CHO^{hRyR2} and CHO^{hRyR2} expressing FKBP12 with rapamycin, there was no change in the magnitude of thapsigargin-induced Ca²⁺ mobilization when compared with untreated cells (Figure 6B, filled bars). In contrast, exposure of cells expressing hRyR2/FKBP12.6 to rapamycin significantly decreased the thapsigargin-releaseable ER Ca²⁺ component (Figure 6B). This suggests that the greatly increased ER Ca²⁺ capacity in CHO^{hRyR2} cells co-expressing FKBP12.6 is probably due to the direct interaction between hRyR2 and FKBP12.6.

Despite similar expression levels of SERCA protein in CHO^{WT} and CHO^{hRyR2} (Figure 3A), we determined a significant increase in SERCA activity in CHO^{hRyR2} cells (when compared with CHO^{WT}), the magnitude of which was proportional to the expression levels of hRyR2 in each cell type (Figure 6C). This result strongly suggests that increased ER Ca²⁺ sequestration in CHO^{hRyR2} is mediated by an associated up-regulation of SERCA activity. Co-expression of FKBP12 or FKBP12.6 had negligible effect on SERCA activity in either CHO^{WT} or CHO^{hRyR2} (Figure 6C), indicating that the marked augmentation in ER Ca²⁺ store in CHO^{hRyR2} after FKBP12.6 expression (Figure 6B) was not associated with a concomitant increase in SERCA activity, indicating that FKBP12.6-mediated superfilling of the ER Ca²⁺ involved other modes of cellular Ca²⁺ sequestration, which remain to be defined.

DISCUSSION

We have, for the first time, expressed the recombinant hRyR2 and demonstrated that it is modulated by interaction with FKBP12.6, which directly regulates Ca²⁺ handling in living CHO^{hRyR2} cells. Full-length recombinant hRyR2 was expressed as an approx. 560 kDa protein, correctly targeted to the ER compartment, folded correctly as determined by *in situ* binding of anti-RyR2 antibodies and fluorescently labelled ryanodine, and formed functional Ca²⁺ release channels in transfected CHO cells. We isolated cell lines (CHO^{#3.2}, CHO^{#3.11} and CHO^{#3.20}) stably expressing discrete levels of hRyR2, which released Ca²⁺ in response to the agonist 4-CMC, the extent of which was proportional to the expression levels of recombinant hRyR2. However, despite several attempts, we did not succeed in isolating a viable cell line that overexpressed high levels of hRyR2, suggesting that increased expression of RyR2 is associated with greater cytotoxicity than that seen with either RyR1 or RyR3 [48,49]. The instability of the permanently expressed rabbit RyR2, which resulted in gross degradation of the recombinant channel in many clonally selected cell lines [50], was probably

associated with its high-level expression and was not seen in our experiments.

We investigated the *in situ* association of hRyR2 with FKBP12.6/FKBP12 in intact CHO^{hRyR2} cells and studied the effect of any protein–protein association on cellular Ca²⁺ homeostasis. Increased cellular redistribution from the cytoplasm to the ER compartments of the cell was observed with FKBP12.6 (but not FKBP12) as the expression levels of hRyR2 increased. This hRyR2-dependent membrane sequestration of FKBP12.6 was reversed by treatment of cells with rapamycin, indicating that our observations *in situ* were indeed due to *bona fide* protein–protein interactions. The finding that there was similar association of FKBP12 with microsomal fractions obtained from CHO^{hRyR2} or RyR-deficient CHO^{WT} cells (Figures 3C and 3E) strongly indicated that FKBP12 association with these fractions was due to its interaction with abundant endogenous IP₃R, an interaction that is widely published [40–44]. Calcium release assays showed that co-expression of FKBP12 had no measurable effect on hRyR2-mediated Ca²⁺ release, whereas the association between hRyR2 and FKBP12.6 markedly decreased 4-CMC-triggered ER Ca²⁺ release (Figure 5). These findings are in agreement with previous results obtained using *in vitro* techniques to determine the specificity of RyR2:FKBP12.6 association [21,51] but significantly extend them by showing that in a cellular context, the interaction occurs dynamically, is modified by their relative expression levels and results in physiologically relevant alteration of intracellular Ca²⁺ handling. Although our results, which were obtained using a non-native CHO cell system, indicated that hRyR2-mediated Ca²⁺ release is not modulated by FKBP12, we cannot exclude the possibility that in cardiac muscle (where FKBP12 expression levels are significantly higher than FKBP12.6 [25]) other RyR2 functions, including the spatial co-ordination of macromolecular complexes [52], are regulated by FKBP12.

In the diseased and failing heart, RyR2 channels are made ‘leaky’ by decreased binding of FKBP12.6 [17,19] and our results showing that FKBP12.6 suppressed hRyR2-mediated Ca²⁺ release are entirely consistent with this model. Over-expression of hRyR2 proportionately augmented agonist-stimulated Ca²⁺ release (Figure 5) and the ER Ca²⁺ store (by increased ER Ca²⁺ sequestration capacity after up-regulation of SERCA activity) (Figure 6), but this increased Ca²⁺ release and sequestration capacity of CHO^{hRyR2} cells did not condition the cell to increased resting [Ca²⁺]_c. Thus the finding that similar resting [Ca²⁺]_c were determined in CHO^{hRyR2} and CHO^{WT} (Figure 5 and relevant text) suggests that in resting CHO^{hRyR2} cells, increased ER Ca²⁺ release (presumably via hRyR2) is compensated for by increased ER Ca²⁺ sequestration via proportionately up-regulated SERCA activity. Although we accept that our heterologous expression system may lack factors implicated in RyR2 regulation *in vivo* [40], this finding that overexpression of hRyR2 did not lead to persistent elevations in resting [Ca²⁺]_c, in agreement with other studies in which ablation of FKBP:RyR interaction did not alter resting [Ca²⁺]_c [23,53], suggests that hRyR2 is subject to a degree of innate regulation that suppresses potentially damaging sustained increases in [Ca²⁺]_c in CHO^{hRyR2} cells.

Our findings regarding the effects of co-expression of FKBP12.6 in CHO^{hRyR2} were intriguing. FKBP12.6 co-expression decreased agonist-induced Ca²⁺ release via hRyR2 (Figure 5), in agreement with the inhibitory nature of FKBP12.6 on hRyR2 described in other studies, yet FKBP12.6 expression concomitantly markedly potentiated the overall ER Ca²⁺ capacity of CHO^{hRyR2} cells. Rapamycin antagonized these effects, thereby strongly indicating a role of FKBP12.6:hRyR2 interaction in these phenomena. Importantly, the rapamycin-sensitive inter-

action of hRyR2:FKBP12.6 induced superfilling of the ER Ca²⁺ store which appeared to be independent of up-regulated SERCA activity. Furthermore, our results show that this FKBP12.6:hRyR2 interaction promoted superfilling of the ER Ca²⁺ store which could not be released after agonist stimulation of hRyR2 using 4-CMC (Figure 5) or caffeine (results not shown). We propose two mechanistic possibilities to explain these observations: (1) FKBP12.6 directly interacts with hRyR2 as a negative regulator of agonist-activated hRyR2-mediated Ca²⁺ release and (2) FKBP12.6:hRyR2 interaction induces ER Ca²⁺ accumulation (SERCA-independent), which is functionally (and possibly spatially) distinct from the hRyR2-agonist (4-CMC)-sensitive Ca²⁺ pool (SERCA-dependent) pre-existing in CHO^{hRyR2} cells. Further work is clearly necessary to determine more precisely the complex ER Ca²⁺ sequestration and release mechanisms underpinning the altered intracellular Ca²⁺ phenotype in CHO^{hRyR2} cells, but our results strongly indicate that FKBP12.6 has a significant impact on hRyR2-mediated Ca²⁺ handling in CHO^{hRyR2} cells. Our studies also indicate that an intact cell-based approach represents a powerful platform for further understanding the complex modulatory protein–protein interactions underlying intracellular Ca²⁺ signalling.

This work was supported by grant nos. PG96091 and PG98169 to F.A.L. from the British Heart Foundation. C.H.G. holds a British Heart Foundation Research Fellowship (FS2000020) and R.S. received a Nuffield Undergraduate Research Bursary (00004G). We thank S. Zissimopoulos for providing the FKBP12 and FKBP12.6 plasmids.

REFERENCES

- Williams, A. J., West, D. J. and Sitsapesan, R. (2001) Light at the end of the tunnel: structures and mechanisms involved in ion translocation in ryanodine receptor channels. *Q. Rev. Biophys.* **34**, 61–104
- Wagenknecht, T., Grassucci, R., Berkowitz, J., Wiederrecht, G. J., Xin, H. B. and Fleischer, S. (1996) Cryoelectron microscopy resolves FK506-binding protein sites on the skeletal muscle ryanodine receptor. *Biophys. J.* **70**, 1709–1715
- Valdivia, H. H. (1998) Modulation of intracellular Ca²⁺ levels in the heart by sorcin and FKBP12, two accessory proteins of ryanodine receptors. *Trends Pharm. Sci.* **19**, 479–482
- Samsó, M., Trujillo, R., Gurrola, G. B., Valdivia, H. H. and Wagenknecht, T. (1999) Three-dimensional location of the imperatoxin A binding site on the ryanodine receptor. *J. Cell Biol.* **146**, 493–499
- Meissner, G. (1994) Ryanodine receptor/Ca²⁺ release channels and their regulation by endogenous effectors. *Annu. Rev. Physiol.* **56**, 485–508
- Ikemoto, N. and Yamamoto, T. (2000) Postulated role of inter-domain interaction within the ryanodine receptor in Ca²⁺ channel regulation. *Trends Cardiovasc. Med.* **10**, 310–316
- Yin, C. C. and Lai, F. A. (2000) Intrinsic lattice formation by the ryanodine receptor calcium release channel. *Nat. Cell Biol.* **2**, 669–671
- Valdivia, H. H., Kaplan, J. H., Ellis-Davies, G. C. R. and Lederer, W. J. (1995) Rapid adaptation of cardiac ryanodine receptors: modulation by Mg²⁺ and phosphorylation. *Science* **267**, 1997–2000
- Xu, L., Eu, J. P., Meissner, G. and Stamler, J. S. (1998) Activation of the cardiac calcium release channel (ryanodine receptor) by poly-S-nitrosylation. *Science* **279**, 234–237
- Eu, J. P., Sun, J., Xu, L., Stamler, J. S. and Meissner, G. (2000) The skeletal muscle calcium release channel: coupled O₂ sensor and NO signaling functions. *Cell (Cambridge, Mass.)* **102**, 499–509
- Takekura, H., Iino, M., Takekura, H., Nishi, M., Kuno, J., Minowa, O., Takano, H. and Noda, T. (1994) Excitation–contraction uncoupling and muscular degeneration in mice lacking functional skeletal muscle ryanodine receptor gene. *Nature (London)* **369**, 556–559
- Takekura, H., Ikemoto, T., Nishi, M., Nishiyama, N., Shimuta, M., Sugitani, Y., Kuno, J., Saito, I., Saito, H., Endo, M. et al. (1996) Generation and characterisation of mutant mice lacking ryanodine receptor type 3. *J. Biol. Chem.* **271**, 19649–19652
- Takekura, H., Komazaki, S., Hirose, K., Nishi, M., Noda, T. and Iino, M. (1998) Embryonic lethality and abnormal cardiac myocytes in mice lacking ryanodine receptor type 2. *EMBO J.* **17**, 3309–3316

- 14 Priori, S. G., Napolitano, C., Tiso, N., Memmi, M., Vignati, G., Bloise, R., Sorrentino, V. and Danieli, G. A. (2001) Mutations in the cardiac ryanodine receptor gene (hRyR2) underlie catecholaminergic polymorphic ventricular tachycardia. *Circulation* **103**, 196–200
- 15 Laitinen, P. J., Brown, K. M., Piippo, K., Swan, H., Devaney, J. M., Brahmabhatt, B., Donarum, E. A., Marino, M., Tiso, N., Viitasalo, M. et al. (2001) Mutations of the cardiac ryanodine receptor (RyR2) gene in familial polymorphic ventricular tachycardia. *Circulation* **103**, 485–490
- 16 Zhao, L., Sebkhii, A., Nunez, D. J. R., Long, L., Haley, C. S., Szpirer, J., Szpirer, C., Williams, A. J. and Wilkins, M. R. (2001) Right ventricular hypertrophy secondary to pulmonary hypertension is linked to rat chromosome 17: evaluation of cardiac ryanodine Ryr2 receptor as a candidate. *Circulation* **103**, 442–447
- 17 Marx, S. O., Reiken, S., Hisamatsu, Y., Jayaraman, T., Burkhoff, D., Roseblit, N. and Marks, A. R. (2000) PKA phosphorylation dissociates FKBP12.6 from the calcium release channel (ryanodine receptor): defective regulation in failing hearts. *Cell* (Cambridge, Mass.) **101**, 365–376
- 18 Ono, K., Yano, M., Ohkusa, T., Kohno, M., Hisaoka, T., Tanigawa, T., Kobayashi, S., Kohno, M. and Matsuzaki, M. (2000) Altered interaction of FKBP12.6 with ryanodine receptor as a cause of abnormal Ca²⁺ release in heart failure. *Cardiovasc. Res.* **48**, 323–331
- 19 Yano, M., Ono, K., Ohkusa, T., Suetsugu, M., Kohno, M., Hisaoka, T., Kobayashi, S., Hisamatsu, Y., Yamamoto, T., Kohno, M. et al. (2000) Altered stoichiometry of FKBP12.6 versus ryanodine receptor as a cause of abnormal Ca²⁺ leak through ryanodine receptor in heart failure. *Circulation* **102**, 2131–2136
- 20 Timerman, A. P., Jayaraman, T., Wiederrecht, G., Onoue, H., Marks, A. R. and Fleischer, S. (1994) The ryanodine receptor from canine heart sarcoplasmic reticulum is associated with a novel FK-506 binding protein. *Biochem. Biophys. Res. Commun.* **198**, 701–706
- 21 Timerman, A. P., Onoue, H., Xin, H. B., Barg, S., Copello, J., Wiederrecht, G. and Fleischer, S. (1996) Selective binding of FKBP12.6 by the cardiac ryanodine receptor. *J. Biol. Chem.* **271**, 20385–20391
- 22 Xin, H. O., Rogers, K., Qi, Y., Kanematsu, T. and Fleischer, S. (1999) Three amino acid residues determine selective binding of FK506-binding protein 12.6 to the cardiac ryanodine receptor. *J. Biol. Chem.* **274**, 15315–15319
- 23 Xiao, R. P., Valdivia, H., Bogdanov, K., Valdivia, C., Lakatta, E. G. and Cheng, H. (1997) The immunophilin FK506-binding protein modulates Ca²⁺ release channel closure in rat heart. *J. Physiol.* **500**, 343–354
- 24 Kaftan, E., Marks, A. R. and Ehrlich, B. E. (1996) Effects of rapamycin on ryanodine receptor/Ca²⁺ release channels from cardiac muscle. *Circ. Res.* **78**, 990–997
- 25 Shou, W., Aghdasi, B., Armstrong, D. L., Guo, Q., Bao, S., Charrng, M. J., Mathews, L. M., Scheider, M. D., Hamilton, S. L. and Matzuk, M. M. (1998) Cardiac defects and altered ryanodine receptor function in mice lacking FKBP12. *Nature* (London) **391**, 489–492
- 26 Barg, S., Copello, J. A. and Fleischer, S. (1997) Different interactions of cardiac and skeletal muscle ryanodine receptors with FK-506 binding protein isoforms. *Am. J. Physiol.* **272**, C1726–C1733
- 27 Jeyakumar, L. H., Ballester, L., Cheng, D. S., McIntyre, J. O., Chang, P., Olivey, H. E., Rollins-Smith, L., Barnett, J. V., Murray, K., Xin, H. B. et al. (2001) FKBP binding characteristics of cardiac microsomes from diverse vertebrates. *Biochem. Biophys. Res. Commun.* **281**, 979–986
- 28 Xin, H. B., Senbonmatsu, T., Cheng, D. S., Wang, Y. X., Copello, J. A., Ji, G. J., Collier, M. L., Deng, K. Y., Jeyakumar, L. H., Magnuson, M. A. et al. (2002) Oestrogen protects FKBP12.6 null mice from cardiac hypertrophy. *Nature* (London) **416**, 334–337
- 29 Tunwell, R. E. A., Wickenden, C., Bertrand, B. M. A., Shevchenko, V. I., Walsh, M. B., Allen, P. D. and Lai, F. A. (1996) The human cardiac muscle ryanodine receptor-calcium release channel: identification, primary structure and topological analysis. *Biochem. J.* **318**, 477–487
- 30 Roderick, H. L., Campbell, A. K. and Llewellyn, D. H. (1997) Nuclear localisation of calreticulin *in vivo* is enhanced by its interaction with glucocorticoid receptors. *FEBS Lett.* **405**, 181–185
- 31 Carmody, M., Mackrill, J. J., Sorrentino, V. and O'Neill, C. (2001) FKBP12 associates tightly with the skeletal muscle type 1 ryanodine receptor, but not with other intracellular calcium release channels. *FEBS Lett.* **505**, 97–102
- 32 Wagenknecht, T., Radermacher, M., Grassucci, R., Berkowitz, J., Xin, H. B. and Fleischer, S. (1997) Locations of calmodulin and FK506-binding protein on the three-dimensional architecture of the skeletal muscle ryanodine receptor. *J. Biol. Chem.* **272**, 32463–32471
- 33 Gryniewicz, G., Poenie, M. and Tsien, R. Y. (1985) A new generation of Ca²⁺ indicators with greatly improved fluorescence properties. *J. Biol. Chem.* **260**, 3440–3450
- 34 Currie, S. and Smith, G. (1999) Enhanced phosphorylation of phospholamban and downregulation of sarco/endoplasmic reticulum Ca²⁺ ATPase type 2 (SERCA) in cardiac sarcoplasmic reticulum from rabbits with heart failure. *Cardiovasc. Res.* **41**, 135–146
- 35 Chu, A., Dixon, M. C., Saito, A., Seiler, S. and Fleischer, S. (1988) Isolation of sarcoplasmic reticulum fractions referable to longitudinal tubules and junctional terminal cisternae from rabbit skeletal muscle. *Methods Enzymol.* **157**, 36–46
- 36 Takeshima, H., Nishimura, S., Matsumoto, T., Ishida, H., Kangawa, K., Minamino, N., Matsuo, H., Ueda, M., Hanaoka, M., Hirose, T. et al. (1989) Primary structure and expression from complementary-DNA of skeletal-muscle ryanodine receptor. *Nature* (London) **339**, 439–445
- 37 Kukkonen, J. P., Lund, P. E. and Akerman, K. E. (2001) 2-Aminoethoxydiphenyl borate reveals heterogeneity in receptor-activated Ca²⁺ discharge and store-operated Ca²⁺ influx. *Cell Calcium* **30**, 117–129
- 38 Mackrill, J. J., Challiss, R. A. J., O'Connell, D. A., Lai, F. A. and Nahorski, S. R. (1997) Differential expression and regulation of ryanodine receptor and myo-inositol 1,4,5-trisphosphate receptor Ca²⁺ release channels in mammalian tissue and cell lines. *Biochem. J.* **327**, 251–258
- 39 Monkawa, T., Miyawaki, A., Sugiyama, T., Yoneshima, H., Yamamoto-Hino, M., Furuichi, T., Saruta, T., Hasegawa, M. and Mikoshiba, K. (1995) Heterotetrameric complex formation of inositol 1,4,5-trisphosphate receptor subunits. *J. Biol. Chem.* **270**, 14700–14704
- 40 Mackrill, J. J. (1999) Protein-protein interactions in intracellular Ca²⁺-release channel function. *Biochem. J.* **337**, 345–361
- 41 Cameron, A. M., Nucifora, F. C., Fung, E. T., Livingstone, D. J., Aldape, R. A., Ross, C. A. and Snyder, S. H. (1997) FKBP12 binds the inositol 1,4,5-trisphosphate receptor at leucine-proline (1400–1401) and anchors calcineurin to this FK506-like domain. *J. Biol. Chem.* **272**, 27582–27588
- 42 Cameron, A. M., Steiner, J. P., Sabatini, D. M., Kaplin, A. I., Walensky, L. D. and Snyder, S. H. (1995) Immunophilin FK506 binding protein associated with inositol 1,4,5-trisphosphate receptor modulates calcium flux. *Proc. Natl. Acad. Sci. U.S.A.* **92**, 1784–1788
- 43 Snyder, S. H., Sabatini, D. M., Lai, M. M., Steiner, J. P., Hamilton, G. S. and Suzdak, P. D. (1998) Neural actions of immunophilin ligands. *Trends Pharm. Sci.* **19**, 21–26
- 44 Bultynck, G., De Smet, P., Rossi, D., Callewaert, G., Missiaen, L., Sorrentino, V., De Smedt, H. and Parys, J. B. (2001) Characterization and mapping of the 12 kDa FK506-binding protein (FKBP12)-binding site on different isoforms of the ryanodine receptor and of the inositol 1,4,5-trisphosphate receptor. *Biochem. J.* **354**, 413–422
- 45 Zorzato, F., Scutari, E., Tegazzin, V., Clementi, E. and Treves, S. (1993) Chlorocresol: an activator of ryanodine receptor mediated Ca²⁺ release. *Mol. Pharmacol.* **44**, 1192–1201
- 46 Fessenden, J. D., Wang, Y., Moore, R. A., Chen, S. R. W., Allen, P. D. and Pessah, I. N. (2000) Divergent functional properties of ryanodine receptor types 1 and 3 expressed in a myogenic cell line. *Biophys. J.* **79**, 2509–2525
- 47 Du, G. G. and MacLennan, D. H. (1998) Functional consequences of mutations of conserved, polar amino acids in transmembrane sequences of the Ca²⁺ release channel (ryanodine receptor) of rabbit skeletal muscle sarcoplasmic reticulum. *J. Biol. Chem.* **273**, 31867–31872
- 48 Du, G. G., Imredy, J. P. and MacLennan, D. H. (1998) Characterization of recombinant rabbit cardiac and skeletal muscle Ca²⁺ release channels (ryanodine receptors) with a novel [³H]ryanodine binding assay. *J. Biol. Chem.* **273**, 33259–33266
- 49 Manunta, M., Rossi, D., Simeoni, I., Butelli, E., Rومانin, C., Sorrentino, V. and Schindler, H. (2000) ATP-induced activation of expressed RyR3 at low free calcium. *FEBS Lett.* **471**, 256–260
- 50 Bhat, M. B., Hayek, S. M., Zhao, J., Zang, W., Takeshima, H., Weir, W. G. and Ma, J. (1999) Expression and functional characterization of the cardiac muscle ryanodine receptor Ca²⁺ release channel in Chinese hamster ovary cells. *Biophys. J.* **77**, 808–816
- 51 Timerman, A. P., Ogunbumni, E., Freund, E., Wiederrecht, G., Marks, A. R. and Fleischer, S. (1993) The calcium release channel of sarcoplasmic reticulum is modulated by FK506 binding protein. *J. Biol. Chem.* **268**, 22992–22999
- 52 Marks, A. R., Marx, S. O. and Reiken, S. (2002) Regulation of ryanodine receptors via macromolecular complexes: a novel role for leucine/isoleucine zippers. *Trends Cardiovasc. Med.* **12**, 166–170
- 53 Weidelt, T. and Isenberg, G. (2000) Augmentation of SR Ca²⁺ release by rapamycin and FK506 causes K⁺-channel activation and membrane hyperpolarization in bladder smooth muscle. *Br. J. Pharmacol.* **129**, 1293–1300